Widely varying giant Goos–Hänchen shifts from Airy beams at nonlinear interfaces

Pedro Chamorro-Posada,[1,*] Julio Sánchez-Curto,[1] Alejandro B. Aceves,[2] and Graham S. McDonald[3]

[1]*Departamento de Teoría de la Señal y Comunicaciones e Ingeniería Telemática, Universidad de Valladolid, ETSI Telecomunicación, Paseo Belén 15, 47011 Valladolid, Spain*

[2]*Department of Mathematics, Southern Methodist University, Clements Hall 221, Dallas, Texas 75275, USA*

[3]*Joule Physics Laboratory, School of Computing, Science and Engineering, Materials and Physics Research Centre, University of Salford, Salford M5 4WT, UK*

**Corresponding author: pedcha@tel.uva.es*

Received December 9, 2013; revised January 16, 2014; accepted January 20, 2014; posted January 24, 2014 (Doc. ID 202745); published March 5, 2014

We present a numerical study of the giant Goos–Hänchen shifts (GHSs) obtained from an Airy beam impinging on a nonlinear interface. To avoid any angular restriction associated with the paraxial approximation, the analysis is based on the nonlinear Helmholtz equation. We report the existence of nonstandard nonlinear GHSs displaying an extreme sensitivity to the input intensity and the existence of multiple critical values. These intermittent and oscillatory regimes can be explained in terms of competition between critical coupling to a surface mode and soliton emission from the refracted beam component and how this interplay varies with localization of the initial Airy beam.

OCIS codes: (190.0190) Nonlinear optics; (190.3270) Kerr effect; (190.4350) Nonlinear optics at surfaces; (190.6135) Spatial solitons.

http://dx.doi.org/10.1364/OL.39.001378

Airy beams [1] have remarkable properties, such as their self-healing capabilities [2], that make them very attractive for applications ranging from linear optical communications [3] to those of the high-intensity nonlinear optical regime [4]. Ideal nondiffracting self-bending optical Airy beams have infinite energy, and some sort of truncation is required to obtain solutions that can be used in practice. Finite energy Airy beams keep the main properties of their ideal counterparts only for a limited propagation distance. Among the various alternatives that have been put forward as finite energy Airy beams, we will use in this work the exponential apodization of the initial beam profile proposed in [5].

The refraction and reflection of Airy beams at linear interfaces were addressed in [6]. Here, we study the behavior of finite energy Airy beams at a linear-nonlinear interface close to the critical angle for total internal reflection. In this setup, an enhancement of the Goos–Hänchen shift (GHS) [7] can be obtained due to the coupling to nonlinear surface modes. This giant or nonlinear GHS was first described in [8] for Gaussian beams and later studied analytically, for nonlinear interfaces, using an equivalent-particle description of optical solitons [9]. Recent experiments using nematic liquid crystals [10,11] demonstrated the controllable nonlinear refraction of optical solitons. The use of a Helmholtz theory for optical solitons [12–14] permitted interface studies without the angular restrictions imposed by the paraxial approximation and revealed new related phenomena [15].

When a Gaussian beam impinges on a nonlinear interface at a fixed angle of incidence [8], the dependence of the total internal reflection angle on the nonlinear refractive index results in the existence of a critical intensity for the coupling to a surface mode. The giant GHS is defined at intensities smaller and close to this critical value that corresponds to the position of a vertical asymptote. The same behavior is found for the interaction of a soliton with a nonlinear interface [9,15].

However, the Airy initial condition has richer phase and amplitude structures, when compared with a Gaussian or a soliton beam, that are intimately related to its self-bending nature. We report that the coupling of the incident Airy beam to the surface mode can exhibit multiple critical values and wide variations in the giant GHS from relatively small changes in the incident beam intensity, producing oscillatory or even intermittent giant GHS regimes. This extreme sensitivity to the field intensity could be used for sensing applications. At larger intensities, we find the simultaneous generation of refracted soliton beams and a reflected component that is subject to the same type of complex interactions with the interface.

We consider a plane boundary separating two media, $l = 1,\ 2$, with refractive indices $n_l^2 = n_{0,l}^2 + n_{\mathrm{NL},l}^2$ and $n_{\mathrm{NL},l}^2 = \gamma_l |E|^2$. The nonlinear Helmholtz equation describing the evolution of a TE polarized optical field $E(x,z) = E_0 u(x,z)\exp(jkn_0 z)$ can be written, in terms of its complex envelope $u(x,z)$, as [12,13]

$$\kappa \frac{\partial^2 u}{\partial \zeta^2} + j\frac{\partial u}{\partial \zeta} + \frac{1}{2}\frac{\partial^2 u}{\partial \xi^2} - \frac{\Delta_l}{4\kappa}u + \alpha_l |u|^2 u = 0, \qquad (1)$$

where $\Delta_l = 1 - (n_{0l}/n_0)^2$, n_0 is an arbitrary reference refractive index, and $4\kappa\alpha_l = \gamma_l E_0^2/n_o^2$ is the ratio of the nonlinear and linear refractive indices [16]. The transverse and longitudinal scalings in $\xi = x/X_0$ and $\zeta = z/Z_0$ are chosen such that $Z_0 = kn_0 X_0^2$ is the Rayleigh range of a hypothetical input Gaussian beam of width X_0. $\kappa = X_0^2/(2Z_0^2)$ keeps the information about the scalings used and permits rewriting any particular solution of the normalized equation back in terms of the laboratory coordinates. This nonparaxiality parameter [12]

$\kappa = ((\lambda_0/n_0)/X_0)^2/(8\pi^2)$ will be very small for paraxial propagation situations. The paraxial approximation amounts to neglecting the first term in Eq. (1), whereby a nonlinear Schrödinger (NLS) equation describes the evolution of the optical beam. Once the nonparaxiality parameter κ is fixed, we adjust the nonlinear refractive index mismatch by varying a single parameter α. This could correspond to a change of either the input beam intensity or the nonlinearity of the medium.

We assume the $l = 1$ incidence medium to be linear, and we set its refractive index as the reference value for the whole study. Therefore, we use $\Delta_1 = 0$ and $\alpha_1 = 0$ in Eq. (1). The refraction of the incident beam takes place at the planar boundary with a focusing Kerr nonlinear medium $\alpha_2 = \alpha > 0$, such that the discontinuity in the linear refractive indices should correspond to (linear) internal refraction $\Delta_2 = \Delta > 0$.

We consider an input beam propagating on axis, with an initial transverse profile

$$u(\xi, \zeta = 0) = Ai(\xi + \xi_p)\exp(a(\xi + \xi_p)) \qquad (2)$$

that corresponds to the initial condition of a finite energy accelerating Airy beam [5]. The angular spectrum of this beam has a width of order $1/\sqrt{2a}$ (that, as it has been noted in [17], decreases as its localization at the launch point increases). Therefore, a paraxial description of the initial propagation of the input beam launched along the optical axis in the incidence medium is adequate provided that $a \gg \kappa$ since the maximum transverse wavenumber in the normalized frame [12] is $1/\sqrt{2\kappa}$. The asymptotic paraxial evolution from Eq. (2) can be accurately approximated by a Gaussian-like term [17] and, therefore, a behavior similar to the corresponding incident Gaussian mode could be expected in this regime.

The intrinsic curvature of the input beam hinders a precise definition of the angle of incidence itself. We base our analysis on the Helmholtz equation [14] and, in order to adjust the incidence conditions, we exploit the associated angular freedom to rotate the interface by an inclination angle θ around a pivoting point at (ξ_0, ζ_0) while the input condition is kept fixed. The use of the full Helmholtz framework also permits one to unambiguously map a transverse shift V in the normalized frame to a physical angle through the nonparaxial parameter κ, using $\theta = \arctan(\sqrt{2\kappa}V)$ [12]. For each set of (a, ζ_0, θ), α is varied starting from $\alpha = 0$; this corresponds, in an associated experimental setup, to a progressive increase of the input beam power. We consider a value of $\Delta = 0.01$ and $\kappa = 0.001$ that amounts to an FWHM of six optical wavelengths. This value has been extensively used in previous analyses and provides a guarantee of the validity of the scalar approximation [12–16].

Perfectly collimated nonlinear waves with planar phase fronts, such as soliton beams or nonlinear plane waves, admit a precisely defined critical angle that can be calculated through a nonlinear Snell's law obtained by phase matching of the solution on each side of the interface [8,9,13]. On the contrary, the complex phase structure of an input Airy condition, linked to its bending nature, imposes the requirement of a numerical approach for the identification of the critical input conditions. A preliminary broad numerical survey permitted identification of the relevant parameter regions that were later studied in a systematic way. The values chosen for a are 0.1, 0.2, 0.3, 0.4, and 0.6. The input beam is defined with $\xi_p = 3$, two values are considered for the interface inclination, $\theta = 1°$ and $\theta = 2°$, ζ_0 takes values from 0 to 12, always with $\xi_0 = 0$, and propagation over a total normalized length of $\zeta = 30$ is considered in all cases.

The value of the localization parameter a is central for the behavior of the Airy beam at the interface. The numerical results suggest the existence of a minimum value of a for the observation of a GHS. Even for $a = 0.1$, a nonlinear GHS is found only at the smallest tilt angle $\theta = 1°$ and when the interface is very close to the launch plane. For this parameter range ($a = 0.1$, $\theta = 1°$) two distinct scenarios can be clearly identified: for $\zeta_0 = 0$ [Figs. 1(a)–1(c)], as α increases toward a critical value, the interaction with the nonlinear interface is very similar to that of Gaussian [8] or soliton beams [9,15] experiencing a giant GHS. When this critical α is exceeded, a refracted soliton is generated in the second medium. If the interface is moved farther to $\zeta_0 = 4$ [Figs. 1(d) and 1(e)] the refracted beam component results in the eventual emission of a soliton in the second medium, in a very similar fashion to that found for the propagation of an Airy beam in a homogeneous nonlinear medium [18].

In Fig. 2 we use the GHS, defined as the distance traveled by the peak of the beam in the second medium, versus the nonlinear mismatch α to analyze the results.

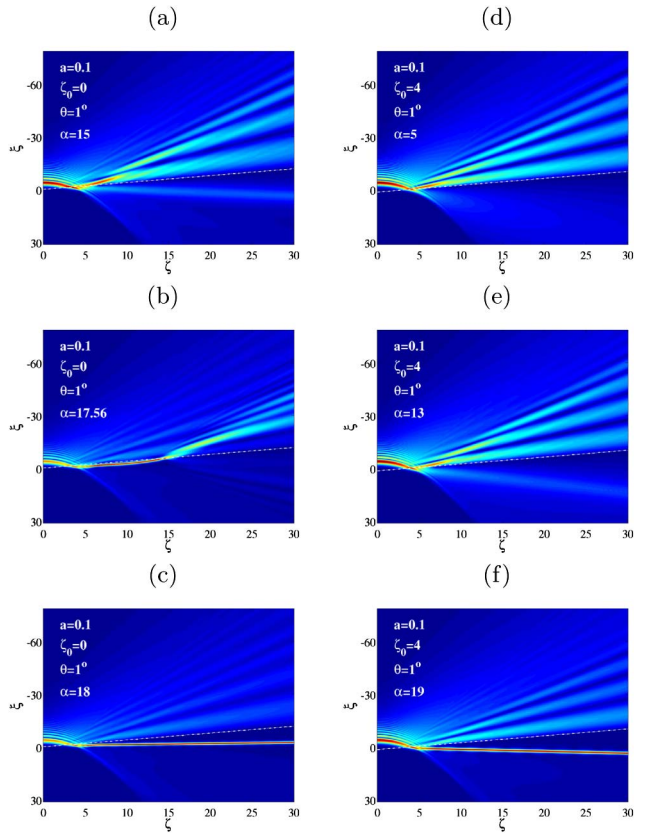

Fig. 1. (a)–(c) Typical sequence in the critical coupling to a surface mode and giant GHS. (d)–(f) Typical soliton shedding sequence as α increases. In both cases $a = 0.1$.

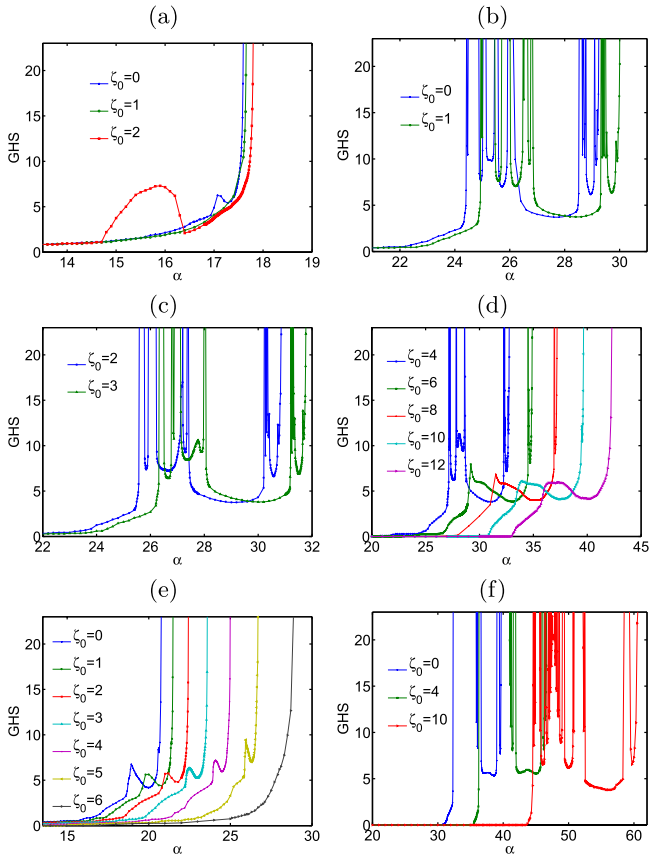

Fig. 2. GHS for different values of ζ_0 and (a) $a = 0.1$ $\theta = 1°$, (b)–(d) $a = 0.2$ $\theta = 1°$, (e) $a = 0.2$ $\theta = 2°$, and (f) $a = 0.3$ $\theta = 1°$.

The maximum GHS shown is limited by the total length of the computation window. The oscillation in the GHS curves displayed in Fig. 2(a) for $\zeta_0 = 2$ can be interpreted as the result of the competition between the two effects: the coupling to a surface mode (giant GHS) and the soliton emission from the refracted beam component.

The effect is far more pronounced when a is increased to 0.2 and 0.3 [Figs. 2(b)–2(f)] where the oscillations in the GHS (Fig. 3) can turn into intermittency regions (Fig. 4), in which the giant GHS effect appears and disappears as α is varied. This multiplicity of critical values resembles the coupling to Tamm waves at an interface with a structured material [19]. While there is a boundary separating two media, each is homogeneous; it is then that the unique oscillatory profile of the Airy beam combined with the nonlinear property of the dielectric to the right of the interface induces both the excitement of a surface wave and the Tamm-like effect.

As a is further increased, the oscillations of the Airy beams are largely diminished and the solutions become closer to their asymptotic Gaussian beam even at small distances to the launch plane, and a behavior close to that of Gaussian input [8] is found for most cases.

Figures 2(b)–2(d) show the results corresponding to $a = 0.2$ at $\theta = 1°$. Intermittency is then clearly observed in all the cases with $\zeta_0 \leq 8$, whereas oscillatory results are found for larger values. When $a = 0.2$ and $\theta = 2°$ [Fig. 2(e)], oscillatory GHS is found for values of ζ_0 up

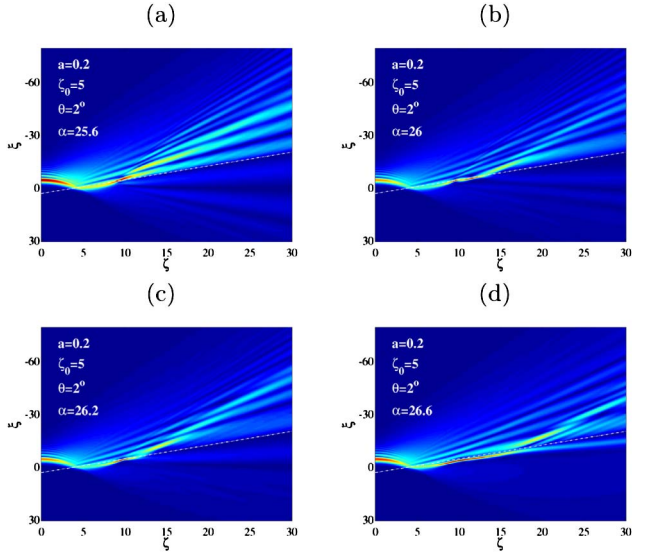

Fig. 3. Oscillations of giant GHS at $\theta = 2°$, $a = 0.2$, and $\zeta_0 = 5$.

to 5 and the oscillations cease at $\zeta_0 = 6$. The soliton shedding process dominates at larger values.

Figure 2(f) shows the giant GHS for $a = 0.3$ and $\theta = 1°$: different intermittency bands are found for all values of ζ_0. When $\theta = 2°$, intermittent GHS is found for $\zeta_0 = 0$ and 1 and giant GHS with oscillations with α for ζ_0 ranging from 2 to 5. If ζ_0 is further increased, after an oscillatory region the critical coupling to a surface mode is superseded by soliton shedding phenomena.

When $a = 0.4$ giant GHS with intermittency is observed when $\theta = 1°$ for all values of ζ_0. For $a = 0.4$ and $\theta = 2°$, intermittent giant GHS is found when ζ_0 is smaller or equal to 5 and oscillatory GHS at $\zeta_0 = 6$. For larger values, the behavior is similar to that of $a = 0.3$ and $\theta = 2°$ at the largest values of ζ_0.

In general, one can observe how the decrease of the peak intensity of the finite energy input Airy beams due to diffraction tends to shift the critical coupling

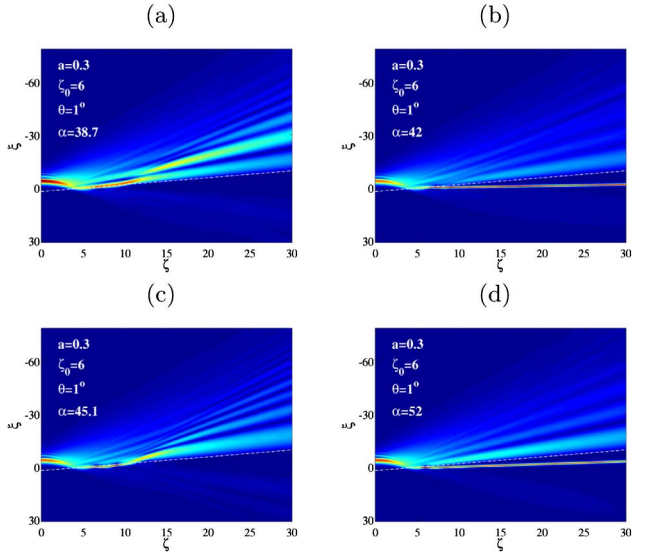

Fig. 4. Setup of an intermittent GHS at $a = 0.3$, $\theta = 1°$, and $\zeta_0 = 6$.

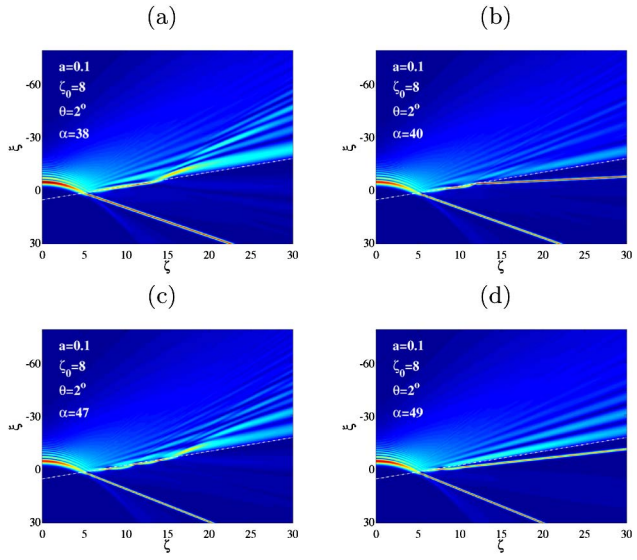

Fig. 5. Intermittent GHS sequence for the second emitted soliton.

features to larger values of α as the interface is moved to larger ζ_0. Even though the results for larger values of α typically resemble those corresponding to an input Gaussian condition, quite remarkably, intermittency is also found for $a = 0.6$, $\theta = 2°$, and $\zeta_0 \geq 8$ at very large values of α.

At larger values of α, one can find the emission of a second soliton in the nonlinear medium and its competing critical coupling to a surface mode that produces the previously described type of oscillatory and/or intermittent GHS with the simultaneous emission of the primary soliton, as shown in Fig. 5.

Some of the results presented involve large values of α. We have performed similar analyses at these values of α and analogous input intensities using input Gaussian beams without observing any intermittent or oscillatory GHS. The accuracy of the numerical results has been checked by reducing the propagation and transverse discretization steps by a factor of 4 for a number of cases at particularly large values of α, without observing any change in the results. We have also studied some parameter ranges using the paraxial NLS equation obtained when the first term in Eq. (1) is neglected, with the result that the same qualitative behavior is observed but with significant quantitative differences.

This work has been funded by the Spanish MICINN, project number TEC2012-21303-C04-04, and Junta de Castilla y León, project number VA300A12-1.

References

1. M. V. Berry and N. L. Balazs, Am. J. Phys. **47**, 264 (1979).
2. J. Broky, G. A. Siviloglou, A. Dogariu, and D. N. Christodoulides, Opt. Express **16**, 12880 (2008).
3. Y. Gu and G. Gbur, Opt. Lett. **35**, 3456 (2010).
4. P. Polynkin, M. Kolesik, J. V. Moloney, G. A. Siviloglou, and D. N. Christodoulides, Science **324**, 229 (2009).
5. G. A. Siviloglou and D. N. Christodoulides, Opt. Lett. **32**, 979 (2007).
6. I. D. Chremmos and N. K. Efremidis, J. Opt. Soc. Am. A **29**, 861 (2012).
7. F. Goos and H. Hänchen, Ann. Phys. **1**, 333 (1947).
8. W. J. Tomlinson, J. P. Gordon, P. W. Smith, and A. E. Kaplan, Appl. Opt. **21**, 2041 (1982).
9. A. B. Aceves, J. V. Moloney, and A. C. Newell, Phys. Rev. A **39**, 1809 (1989).
10. M. Peccianti, A. Dyadyusha, M. Kaczmarek, and G. Assanto, Nat. Phys. **2**, 737 (2006).
11. M. Peccianti, G. Assanto, A. Dyadyusha, and M. Kaczmarek, Opt. Lett. **32**, 271 (2007).
12. P. Chamorro-Posada, G. S. McDonald, and G. H. C. New, J. Mod. Opt. **45**, 1111 (1998).
13. J. Sánchez-Curto, P. Chamorro-Posada, and G. S. McDonald, Opt. Lett. **32**, 1126 (2007).
14. P. Chamorro-Posada, G. S. McDonald, and G. H. C. New, Opt. Commun. **192**, 1 (2001).
15. J. Sánchez-Curto, P. Chamorro-Posada, and G. S. McDonald, Opt. Lett. **36**, 3605 (2011).
16. P. Chamorro-Posada and G. S. McDonald, J. Nonlinear Opt. Phys. Mater. **21**, 1250031 (2012).
17. P. Chamorro-Posada, J. Sánchez-Curto, A. B. Aceves, and G. S. McDonald, "On the asymptotic evolution of finite energy Airy wavefunctions," http://www.arxiv.org/abs/1305.3529.
18. Y. Fattal, A. Rudnick, and D. M. Marom, Opt. Express **19**, 17298 (2011).
19. H. Maaba, M. Faryadb, and A. Lakhtakiab, J. Mod. Opt. **60**, 355 (2013).